

# Journal of Materials Chemistry A

Accepted Manuscript



This article can be cited before page numbers have been issued, to do this please use: N. chen, L. Qin and Q. Pan, *J. Mater. Chem. A*, 2018, DOI: 10.1039/C8TA00760H.

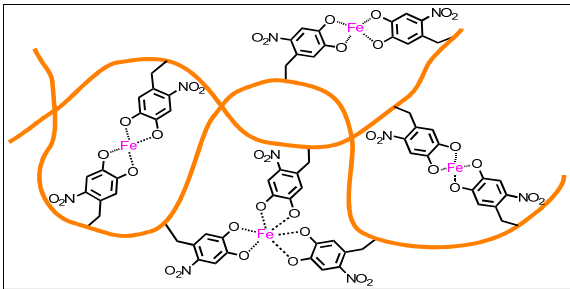


This is an Accepted Manuscript, which has been through the Royal Society of Chemistry peer review process and has been accepted for publication.

Accepted Manuscripts are published online shortly after acceptance, before technical editing, formatting and proof reading. Using this free service, authors can make their results available to the community, in citable form, before we publish the edited article. We will replace this Accepted Manuscript with the edited and formatted Advance Article as soon as it is available.

You can find more information about Accepted Manuscripts in the [author guidelines](#).

Please note that technical editing may introduce minor changes to the text and/or graphics, which may alter content. The journal's standard [Terms & Conditions](#) and the ethical guidelines, outlined in our [author and reviewer resource centre](#), still apply. In no event shall the Royal Society of Chemistry be held responsible for any errors or omissions in this Accepted Manuscript or any consequences arising from the use of any information it contains.



A mussel-inspired strong and stiff polymer exhibits healability, renewability, anti-flammability and solvent-tolerance.

## Mussel-inspired healing of strong and stiff polymer

Ning Chen, Liming Qin, Qinmin Pan\*

(State Key Laboratory of Robotics and Systems, School of Chemistry and Chemical Engineering, Harbin Institute of Technology, Harbin 150001, *P. R. China*)

## Abstract

Self-healability will greatly improve the reliability, service life and maintenance of synthetic materials. However, it remains a big challenge to realize self-healing of a strong and stiff polymer due to its poor molecular mobility. Inspired by hardness and self-healability of the cuticle of mussel byssal threads, here we demonstrate that a stiff and strong polymer can heal itself through dynamic metal-ligand interaction. The polymer is comprised of nitrocatechol-substituted chitosan cross-linked by catechol-Fe complexation, which exhibits a tensile strength ( $63.6 \pm 2.2$  MPa) and an elastic modulus ( $862.6 \pm 31$  MPa) comparable to or even better than those of common engineering plastics. Once suffering from multiple physical damages, the stiff polymer is able to recover its configuration integrity and mechanical properties autonomously *via* pH-induced coordination between  $\text{Fe}^{3+}$  and catecholic moiety. Moreover, the polymer also exhibits interesting renewability, flame retardance and solvent-tolerance. Application of the polymer is demonstrated by a weight-bearing test. Our investigation offers a bio-inspired strategy to design healable rigid polymers that have potential applications in various technologic fields.

**Keywords:** stiff polymer, healable, mussel-inspired, dynamic catechol-Fe coordination, pH-induced

## Introduction

Self-healing is an impressive ability that can spontaneously repair mechanical damage, which is common in living organisms. Inspired by this phenomenon, synthesizing self-healable materials had attracted extensive interest over the past decades.<sup>1-3</sup> Compared to its conventional equivalent, a synthetic self-healable material possesses excellent reliability, easy maintenance, long service life, and reduced waste. In terms of self-healing mechanism, there are extrinsic self-healability and intrinsic self-healability. The extrinsic self-healability is realized by pre-storing healing agents such as monomer or catalyst inside microcapsules or microvascular networks.<sup>4,5</sup> In contrast, intrinsically self-healing is mainly based on dynamic covalent bonding (Diels–Alder reaction,<sup>6-8</sup> disulfide,<sup>9-11</sup> cycloaddition reaction,<sup>12,13</sup> radical dimerization reaction,<sup>14</sup> borate ester bonding<sup>15-17</sup> and metal-ligand coordination,<sup>18-21</sup> *etc*) or reversible physical interactions like hydrogen bonding,<sup>22-24</sup> host-guest interaction<sup>25-27</sup> or  $\pi$ - $\pi$  stacking interaction.<sup>28,29</sup> For either extrinsic or intrinsic self-healable material, self-healing behavior takes place only when its polymer chains can diffuse across the broken interface, which means that the mobility of polymer chains is crucial for the self-healability. Actually most of existing self-healable polymers are soft and flexible in order to ensure good chain mobility. However, polymers used in daily life and technological fields are usually strong and rigid, their self-healing remains a big challenge due to poor chain mobility.<sup>30</sup> It is highly desired to achieve stiffness and self-healability simultaneously without conflict through a facile and versatile strategy.

Nature often provides inspiration for designing novel functional materials. Mussel is a kind of marine organism that can fasten itself to almost all kinds of solids in aqueous environments by byssal threads coated with a proteinaceous cuticle.<sup>31,32</sup> The cuticle exhibits not only a mechanical hardness up to ~0.1 GPa but also a breaking strain of 100%, which endows mussel with strong adhesion even in the turbulent intertidal zone.<sup>33</sup> It was recently revealed that the cuticle is rich in the catechol-like amino acid comprising 3,4-dihydroxyphenylalanine (dopa),<sup>34-36</sup> and the coordination of the dopa with a small amount of metal ions, mainly  $\text{Fe}^{3+}$ , accounts for the hardness and

high extensibility.<sup>37-38</sup> More importantly, dopa-metal bonds are apt to spontaneously reform after breaking, enabling the damaged cuticle to heal itself through the regeneration of catechol-Fe complexes.<sup>39-41</sup> Therefore, it is the coordination between catecholic moiety and ferric ion responsible for both hardness and self-healing capability of the cuticle.<sup>42</sup> All these motivate us to realize the healing of a rigid polymer by introducing catechol-Fe coordination into its backbone.

Here we report healing of a stiff and strong polymer *via* a mussel-inspired strategy. The polymer is composed of nitrocatechol-substituted chitosan cross-linked by dynamic catechol-Fe complexation, which exhibits a tensile strength of  $63.6 \pm 2.2$  MPa, elongation of  $53.33 \pm 6$  % and an elastic modulus up to  $862.6 \pm 31$  MPa. Once the polymer is thoroughly cut off, it can spontaneously restore its configuration and mechanical properties *via* pH-induced coordination between  $\text{Fe}^{3+}$  and catecholic moiety. Although the restoration involves slight pressure for the alignment of the cut parts, it is realized autonomously through a microscopic process as that occurs in a living mussel. Therefore, the restoration can be considered as a self-healing process. Given that similar metal-ligand coordination can be introduced to a wide range of polymeric chains, various healable rigid polymers might be synthesized through the bio-inspired strategy reported here.

## Experimental section

### Preparation of the stiff CNC polymer

At first chitosan substituted with nitrocatechol (chitosan-nitrocatechol, CNC) was synthesized through a reductive amination reported in the literatures (Fig. S1, ESI†).<sup>43,44</sup> Then 2 g of CNC was dissolved in 10 mL water and later 10-70 mg of FeCl<sub>3</sub> was slowly added to the resulting solution under stirring. The acidity of the CNC/FeCl<sub>3</sub> solution was adjusted to pH 3 by 0.1 mol L<sup>-1</sup> NaOH solution, giving rise to brown CNC hydrogel. The hydrogel was then shaped in a mold and subsequently dipped in a NaAc buffer (0.5 mol L<sup>-1</sup>, pH = 5.5) for 1 h. After drying at 50 °C, a strong and rigid CNC polymer was obtained.

For the preparation of the CNC filaments, the CNC/FeCl<sub>3</sub> solution was first loaded into a 5 mL plastic syringe with a nozzle of 1.2-2.0 mm in diameter. The hydrogel was then injected into a coagulation bath containing the NaAc buffer *via* a syringe pump at a rate of 0.05-3 mL min<sup>-1</sup>. After coagulation for 60 min, the filaments were taken out from the bath and then dried at 50 °C for 2 h.

### Healing of the CNC polymer

Typically, a CNC bar with the size of 50 mm × 10 mm × 5 mm was first cut into halves by a razor blade. The cut interfaces were wetted by 0.25 mol L<sup>-1</sup> HCl solution for 10 min. The wetted halves were carefully placed in contact for geometric matching. Here only very little pressure was needed for the contact and the matching was evaluated by visual inspection. Later the contact region was wetted by the NaAc buffer for 1 h. The halves autonomously healed into a single unit that could support its own weight. The healed bar was dried at 50 °C for 2 h and then subjected to tensile experiments and microscopic observations.

### Tensile experiments

The original (or healed) CNC filaments with 0.6 mm diameter and 40 mm length were used as testing samples. Two ends of each filament were fixed to the clips of a universal electromechanical testing machine (CREE 8007B). Then the filaments were stretched at a rate of 15 mm s<sup>-1</sup> until breaking. The stress-strain curves of the samples

were recorded and their mechanical healing efficiency ( $\eta$ , %) was determined by the formula  $\eta = T_h/T_o \times 100$ , where  $T_h$  and  $T_o$  are the tensile strength of the healed and the original samples, respectively.

### Regeneration of the CNC polymer

A CNC filament was first cut into small pieces and then dissolved in 10 mL dilute HCl solution (0.25 mol L<sup>-1</sup>). The obtained viscous solution was injected into the NaAc buffer to produce a hydrogel filament. After drying at 50 °C for 2 h, the resulting filament was subjected to tensile experiments to assess its mechanical properties.

### Characterizations

Scanning electron microscopic (SEM) images were recorded by a Zeiss supra 55. Tensile experiments were performed on a universal electromechanical testing machine (Cree 8007B). Optical microscopy observations were conducted on a Phenix PH50-1B43L-A/PL (China). Proton nuclear magnetic resonance (<sup>1</sup>H NMR) was conducted on a Bruker 400. Ultraviolet visible (UV-vis) spectroscopy was performed on a Mapada UV-6100 spectrometer.



## Results and discussion

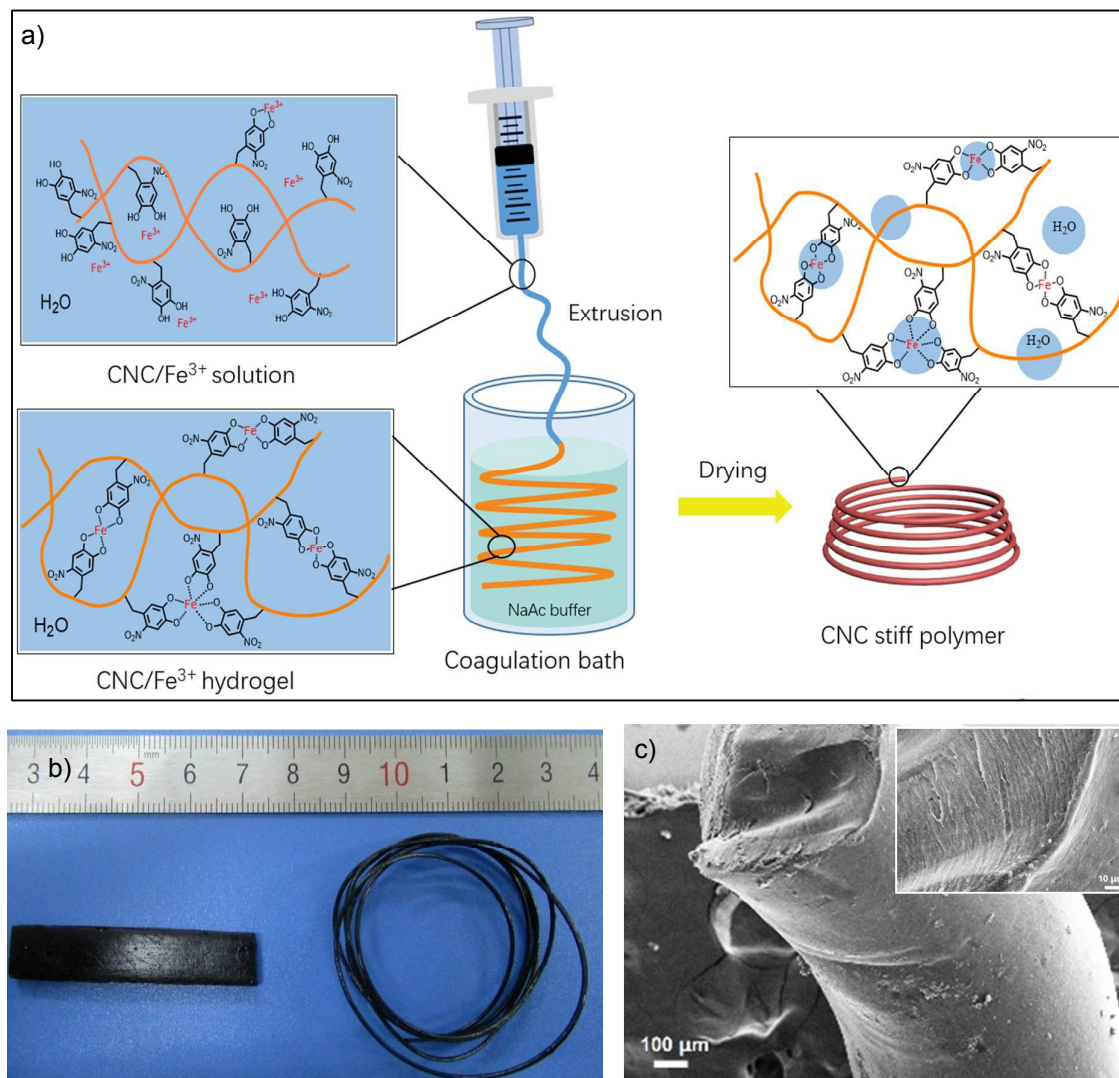


Fig. 1 (a) Synthesis of the stiff CNC polymer. (b) Optical and (c) SEM images of the as-prepared CNC polymer.

The inset is the cross-sectional image.

Fig. 1a illustrates the synthesis of the reported stiff polymer. At first, nitrocatechol was synthesized through a previous process and then it was substituted to chitosan *via* reductive amination (Fig. S1-2, ESI<sup>†</sup>). The obtained polymer (chitosan-nitrocatechol, CNC) was dissolved in a 0.1 mol L<sup>-1</sup> HCl solution containing a small amount of FeCl<sub>3</sub>. As the acidity of the resulting solution was adjusted to pH 5.5, the CNC chains were cross-linked by catechol-Fe coordination to form a brown hydrogel. Finally the hydrogel was dried at 50 °C to produce a strong and stiff CNC polymer (Fig. 1a). The resulting polymer showed a smooth and compact morphology (Fig. 1b-c).

The water content in the CNC polymer was measured to be 3.3 wt% by thermogravimetric analysis (Fig. S3, ESI†).

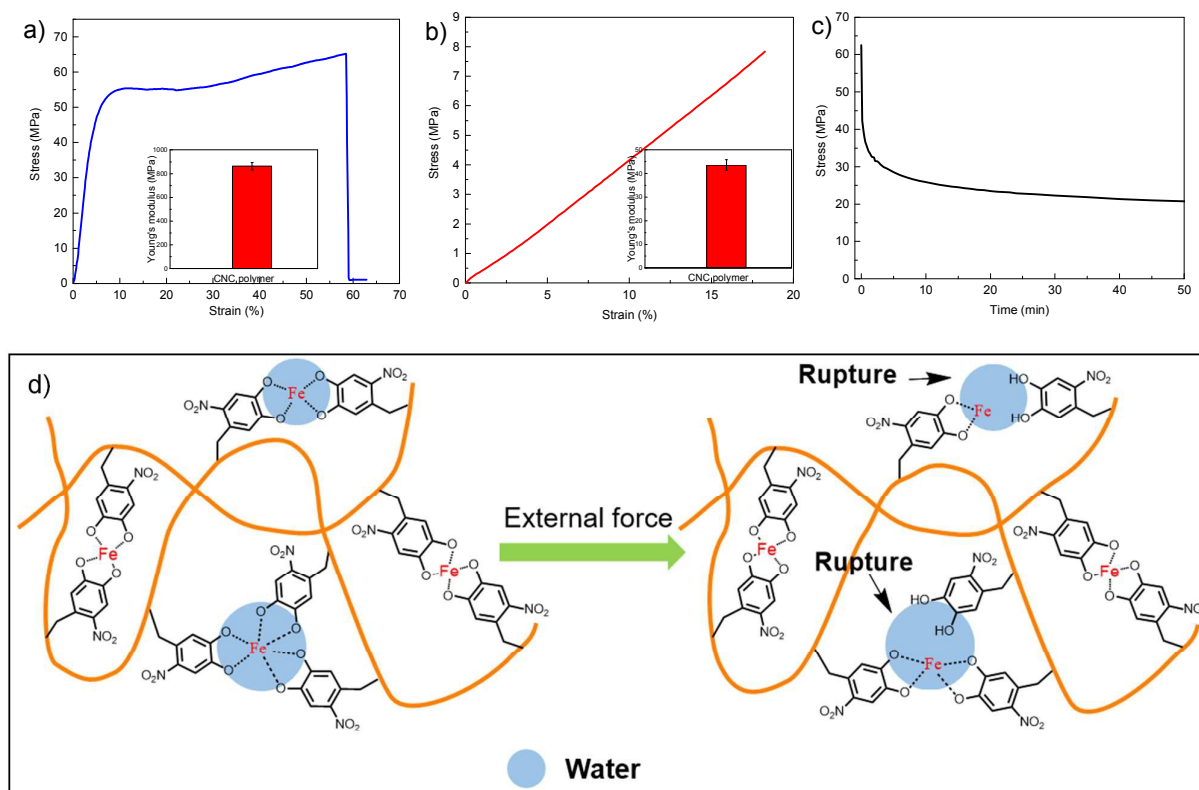


Fig. 2 (a) Tensile stress–strain, (b) compressive stress–strain and (c) stress–relaxation curves of the CNC polymer at 25 °C. The insets are the average Young’s modulus of the four equal samples. (d) Mechanism for the excellent mechanical properties of the polymer. The catechol-Fe coordination serves as sacrificial bonds in the case of mechanical damage.

The mechanical properties of the CNC polymer were evaluated by uniaxial tensile and compressive measurements in ambient environment (25 °C and RH = 25%). For reproducibility, four equal samples were tested at a rate of 15 mm s<sup>-1</sup> for each kind measurement. The results of the tensile experiments are presented in Fig. 2a. The polymer exhibits a tensile strength of 65 MPa and an elastic modulus up to 862.6 ± 31 MPa. Notably, the elongation at break reaches 53.3 ± 6% by applying a tensile strength of 65 MPa, indicating good extensibility. Compressive measurements revealed that the polymer has a compressive modulus of 43.6 ± 2.3 MPa (Fig. 2b).

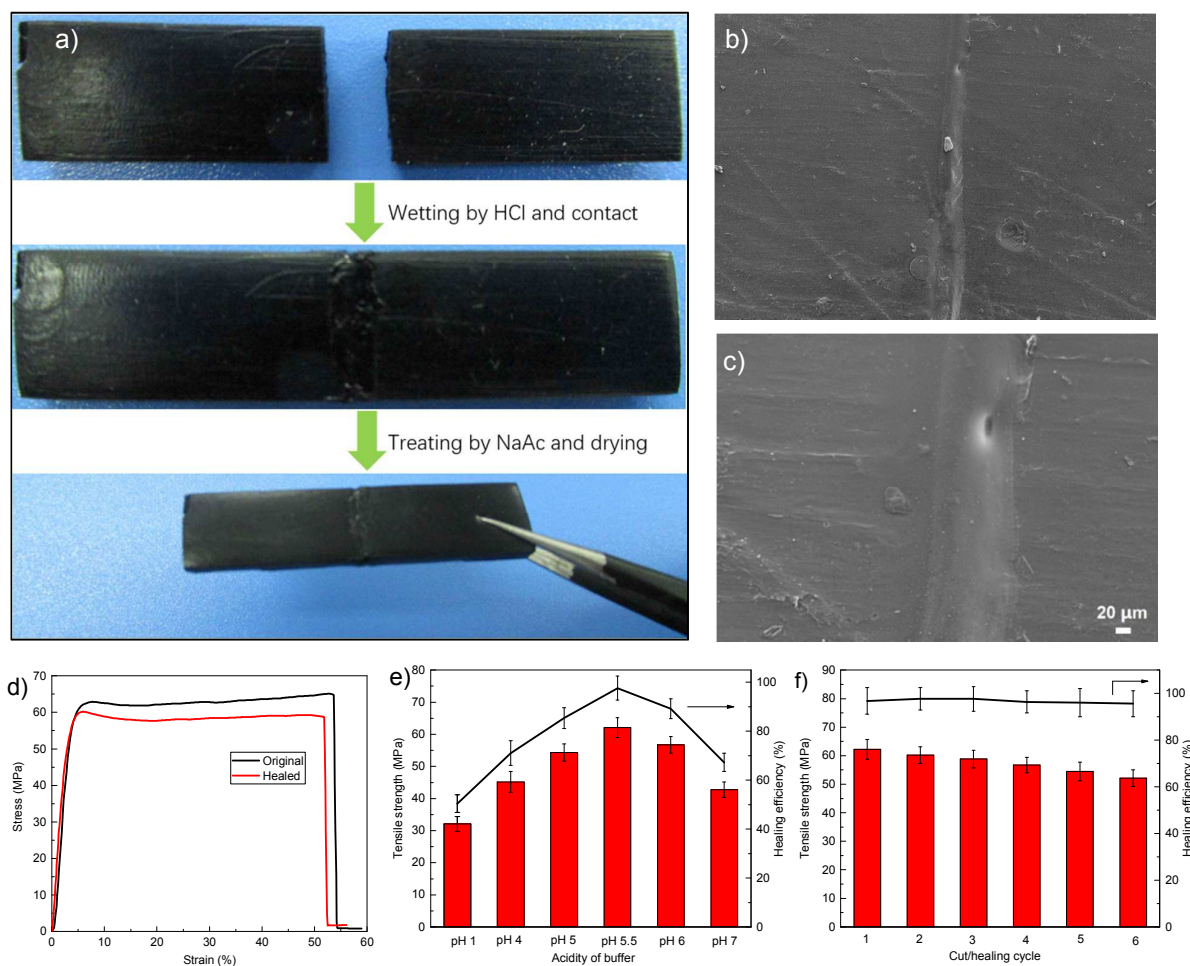
The values are closed to or even better than those of common engineering plastics like polyoxymethylene (POM), polyphenylene Oxide (PPO) and polycarbonate (PC) (Table 1). Stress-relaxation experiments showed that the polymer underwent substantial stress relaxation with time at 25 °C (Fig. 2c). However, the residual stress was still above 20.7 MPa after 50 min relaxation. The outstanding mechanical properties are attributed to the cross-linking of CNC chains by nitrocatechol-Fe complexation. In the presence of trace water, the catechol-Fe coordination exhibits dynamic nature.<sup>45</sup> Once suffering from external force, the coordination ruptures preferentially as a sacrificial bond to dissipate energy and thus prevents the crack to propagate,<sup>18,42,46-48</sup> ensuring the robustness and good extensibility of the polymer. The factors affecting the mechanical properties of the CNC polymer were summarized in Fig. S4-8 of ESI†. It was found that the acidity of the coagulation solutions, the molar ratio of Fe/nitrocatechol, drying temperature and time played an important role in the tensile strength and breaking strain of the resulting polymer. All the results clearly demonstrate that our CNC is a hard and strong polymer with poor chain mobility.

Table 1. Comparison on the mechanical properties of typical engineering plastics.

Engineering plastics	Tensile strength (MPa)	Breaking strain (%)
Nylon-6	51-78	150-250
Polyoxymethylene (POM)	58-70	15-75
Polyphenylene Oxide (PPO)	48-66	35-60
Polycarbonate (PC)	60-88	80-95
Polyphenylene sulfide (PPS)	85-142	2.1-8
polyetheretherketone (PEEK)	~110	20
This work	52-82	8.7-54

Interestingly, the CNC polymer exhibited a pH-induced healing behavior. Here a CNC bar with the size of 50 mm × 10 mm × 5 mm was first severed into halves by a razor blade. The cut interfaces were wetted with a dilute HCl solution (0.25 mol L<sup>-1</sup>, pH = 0.6) and then placed in contact for geometric matching. The contacted pieces were further treated with a NaAc buffer (0.5 mol L<sup>-1</sup>, pH = 5.5) and then dried at 50 °C. After drying for 2 h, the halves merged into a single unit that could withstand its own weight (Fig. 3a). Both visual inspection and optical microscopy observation confirmed that there was almost no gap at the contact region (Fig. 3b), indicating the

healing of the broken sample. We further investigated the mechanical properties of the healed sample by tensile experiments. Fig. 3c compares the stress-strain curves of the sample before and after healing. The healed sample exhibits a tensile strength of 62 MPa. Its mechanical healing efficiency, the ratio of the tensile strength between the healed and original samples, is calculated to be 90%. Moreover, the healed sample also shows a breaking strain (55%) closed to that of its original counterpart. The results confirm efficient recovery of the mechanical properties.



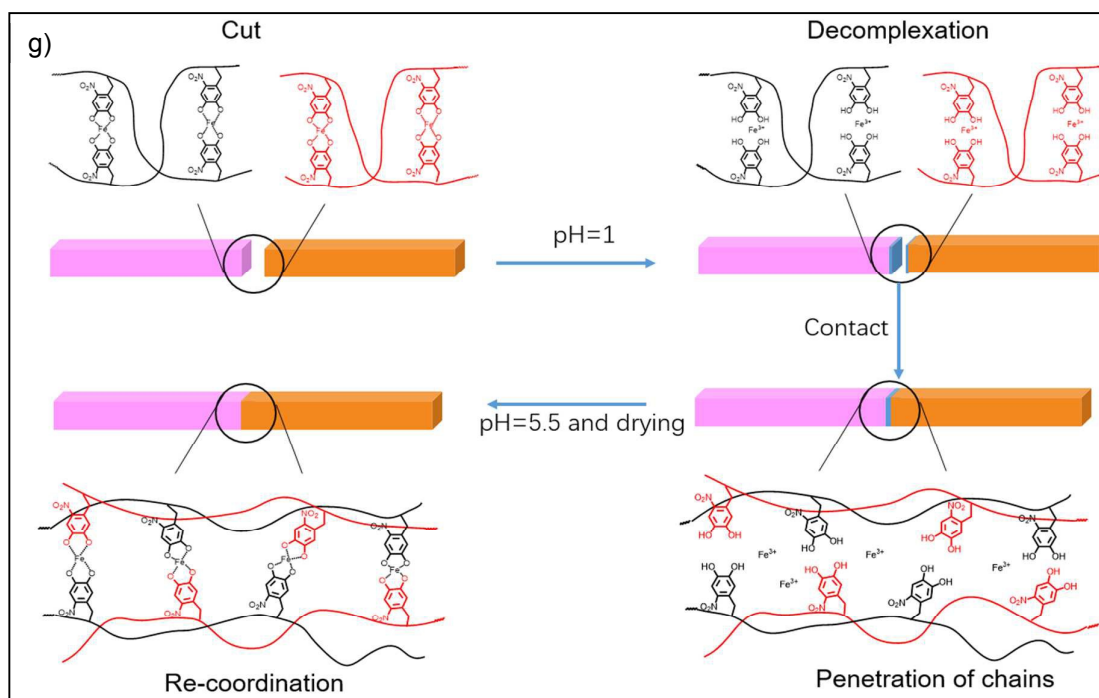


Fig. 3 (a) Optical images show the healing behavior of the CNC polymer. (b) Optical microscopic and (c) SEM images of the healed region. (d) Stress-strain curves of the original and healed CNC samples. (e) Effect of the acidity of the buffers on the mechanical healing efficiency of the CNC samples. (f) Variation of healing efficiency after multiple breaking/healing cycles. (g) Illustration of the healing mechanism of the CNC polymer.

We also found that the pH variation was crucial for the healing behavior. For comparison, CNC samples were first severed and their cut interfaces were wetted by a dilute HCl solution (pH 0.6), NaAc (pH 4-5.5) and KH<sub>2</sub>PO<sub>4</sub> (pH 6-7) buffers, respectively. After the same contact and heat treatment, the resulting samples were investigated by tensile experiments to evaluate their mechanical healing efficiency. Fig. 3d compares the healing efficiency of the CNC samples healed under different conditions. For the sample only treated with the pH 0.6 HCl, it shows a tensile strength of  $32.1 \pm 2.3$  MPa and a healing efficiency of 50.4%. The values are much lower than those of the sample treated with the dilute HCl and then the NaAc buffer. The maximum tensile strength and healing efficiency can be achieved when the polymer is treated by the buffer with pH 5.5. In this case, the healing can take place for at least 6 cycles with an efficiency over 90% (Fig. 3e). The polymer also exhibits a relatively low healing efficiency as the acidity of the buffer is higher than pH 5.5.



The unique healing behavior of the CNC polymer is attributed to pH-induced coordination between nitrocatecholic moiety and  $\text{Fe}^{3+}$ .<sup>41,49-51</sup> When the CNC filament was cut into halves, a large amount of catechol-Fe coordination was cleaved. After the cut interfaces were wetted by the dilute HCl solution, the equilibrium of catechol-Fe coordination shifted to disassociated state, resulting in decomplexation of tris-catechol-Fe chelates. The decomplexation produced abundant free CNC chains that could interpenetrate or entangle at the contact interface. At the pH higher than 4, these free CNC chains were cross-linked again *via* bis- or tris-Fe-catechol coordination between free nitrocatecholic moieties and  $\text{Fe}^{3+}$  (Fig. S5, ESI†),<sup>41,44</sup> leading to the re-construction of the broken CNC network (Fig. 3f). In contrast, the similar re-coordination did not take place for the sample healed only in a strong acidic medium. Notably, the CNC network healed in the  $\text{KH}_2\text{PO}_4$  buffer became fragile because its chains were highly cross-linked in this case.

Nitro substitution significantly affected the healing recyclability of the CNC polymer. To prove the importance, we synthesized chitosan substituted with catechol (chitosan-catechol, CC) as a control sample (Fig. S1, ESI†). The control polymer failed to fully recover its tensile strength and elongation after the same cut/healing operations, exhibiting a mechanical healing efficiency of only 22.6 % (Fig. S9, ESI†). The failure is due to the oxidation of the catecholic moiety into semiquinone or quinone by  $\text{Fe}^{3+}$ .<sup>52-53</sup> The oxidized products are highly reactive,<sup>32</sup> resulting in covalent cross-linking of CC chains. The covalent cross-linking significantly impedes the release of CC chains in the subsequent decomplexation process. On the contrary, the similar oxidation is effectively hindered by the electron-withdrawn nitro group for the CNC polymer.

The strong and stiff CNC polymer was also renewable through the pH variation process. To confirm the renewability, we first crushed the polymer into small pieces and subsequent dissolved them in a dilute HCl solution (Fig. 4a). The resulting solution was extruded into a pH 5.5 NaAc buffer to produce a CNC filament. The regenerated filament also showed a tensile strength of 64.1 MPa and breaking strain of 55.9 % after drying at 50 °C for 2 h (Fig. 4b), which is closed to those of its original counterpart (*i.e.*, 64.9 MPa and 58.5%). The

regeneration greatly reduces the waste and environmental impact. Moreover, the CNC polymer exhibited a flame-retardant property. As shown in Fig. 4c, a CNC filament cannot be ignited even after being treated with a flame for 1 min. In contrast, a polypropylene plate was ignited immediately and the flame propagated quickly with a large amount of drippings (Fig. S10, ESI†). The flame retardance of the CNC polymer mainly lies in high limit oxygen index and charring ability of its chitosan backbone. The former endows the polymer with self-extinguishing property and the later prevents it from melting dripping at high temperature.<sup>54-56</sup> Moreover, the grafted nitrocatecholic moiety acts as a radical scavenger that retards flame propagation.<sup>57,58</sup> The anti-flammability greatly increases the safety of the polymer in the fire.

More interestingly, the CNC could tolerate various organic solvents, although it is a kind of polymeric material. To investigate the solvent tolerance, we treated the CNC filaments with different solvents such as tetrahydrofuran (THF), toluene and dichloromethane for 24 h, and then their stress-strain curves were recorded by tensile experiments. Fig. 4d summarizes the stress strength and elongation of the resulting samples. By comparing the data with those of the original sample, we found that the solvent treatments did not significantly deteriorate the mechanical properties. Moreover, the solvent-treated samples also kept their healing capability (Fig. S11, ESI†). For example, a toluene treated filament recovered both tensile strength and elongation through the same pH-induced coordination processes. The excellent solvent tolerance enables the polymer to be used under harsh conditions.

Application of the healable stiff polymer was demonstrated by a weight-bearing test (Fig. 4e). A CNC filament with the diameter of 0.5 mm was first loaded with 1.0 kg weight. Then additional loading was added slowly until the filament was fractured. The broken filament was treated by pH variation and dried at 50 °C for 2 h allowing for healing. The healed filament could still withstand 1.0 kg loading without breaking. In this case, both original and healed filaments could bear at least 10204 times of their own weight (*i.e.*, 98 mg) and the weight-bearing test was repeatable for multiple times. The excellent mechanical durability together with unique healability allows our

CNC polymer to be a promising material in some special technologic fields including spatial and oceanic science.

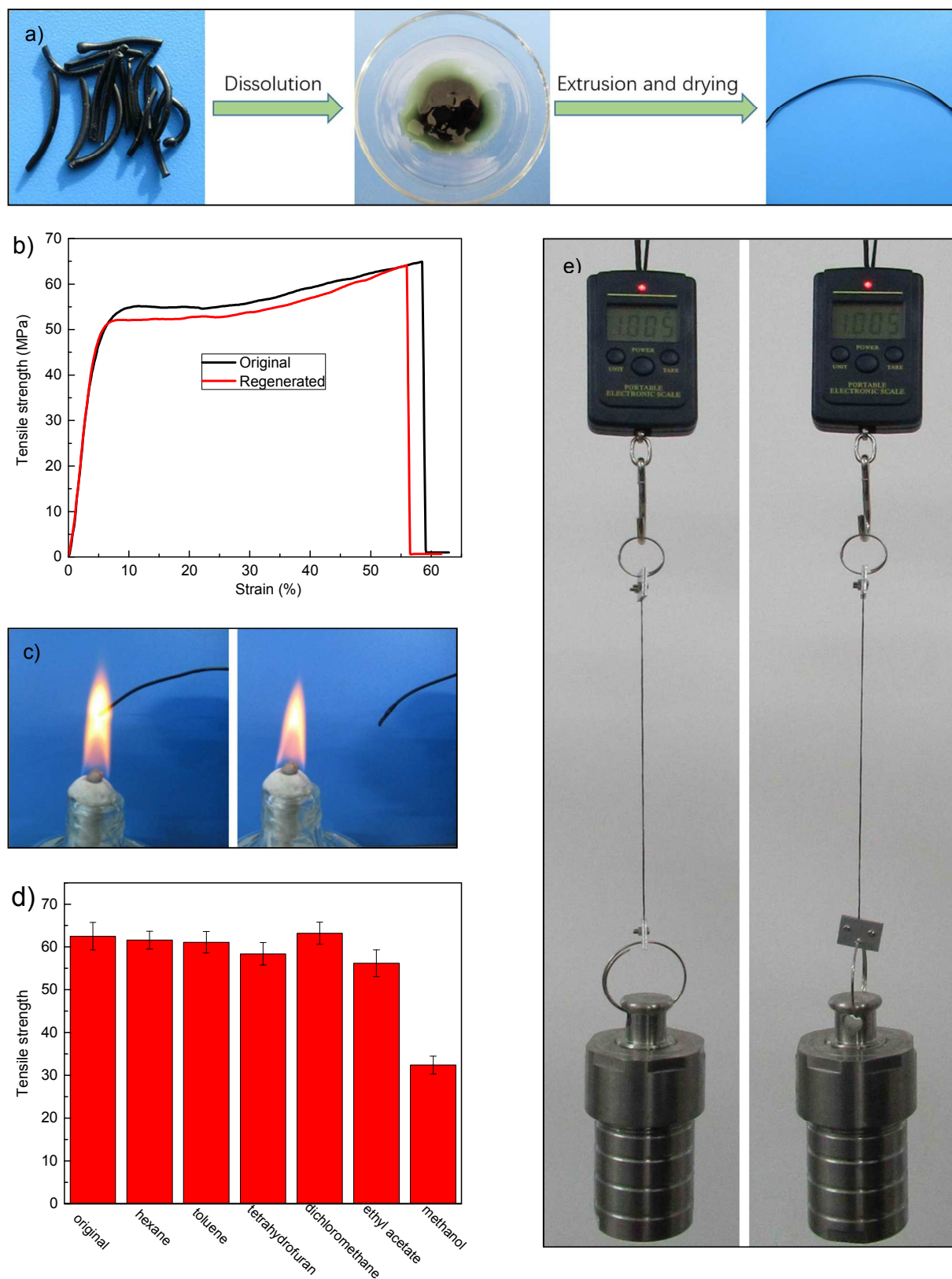


Fig. 4 (a) Optical images show the regeneration of the CNC polymer, and (b) stress-strain curves of the polymer



before and after regeneration. (c) Fire-retardant property of the CNC filament. (d) Tensile strength of the CNC filaments after treating with different solvents for 24 h. (e) Weight-bearing test of the CNC filament with diameter of 500  $\mu\text{m}$  before (left) and after (right) healing.

## Conclusions

In summary, this study demonstrated the healing of a stiff and strong polymer through a mussel-inspired strategy. Although the polymer had hardness comparable to common engineering plastics, it restored its configuration and mechanical properties even after 6 cycles of cutoffs. The restoration is attributed to the increased mobility of its chains *via* decomplexation of Fe-catechol coordination in the acidic media. It was revealed that pH-induced interpolymer cross-linking played an important impact on the healing efficiency and mechanical properties. Moreover, the polymer also exhibited interesting renewability, fire-retardant and solvent-tolerance. This bio-inspired strategy offers a new healing mechanism for rigid polymer through dynamic metal-ligand coordination, which is of scientific and technologic significance.

## Conflicts of interest

There are no conflicts to declare.

## Acknowledgements

This study is financially supported by National Natural Science Foundation of China (51473041) and a self-planned task of the State Key Laboratory of Robotics and System of Harbin Institute of Technology (SKLRS201604C) and Foundation for Innovative Research Groups of the National Natural Science Foundation of China (51521003).

## References

1. E. Palleau, S. Reece, S. C. Desai, M. E. Smith, M. D. *Adv. Mater.*, 2013, **25**, 1589–1592.
2. V. K. Thakur, M. R. Kessler, *Polymer*, 2015, **69**, 369–383.
3. P. W. Richard, *Soft Matter*, 2008, **4**, 400–418.
4. S. R. White, J. S. Moore, N. R. Sottos, B. P. Krull, W. A. S. Cruz, R. C. R. Gergely, *Science*, 2014, **344**, 620–623.
5. K. S. Toohey, N. R. Sottos, J. A. Lewis, J. S. Moore, S. R. White, *Nat. Mater.*, 2007, **6**, 581–585.
6. X. X. Chen, M. A. Dam, K. Ono, A. Mal, H. B. Shen, S. R. Nutt, K. Sheran, F. Wudl, *Science*, 2002, **295**, 1698–1702.
7. Y. Heo, H. A. Sodano, *Adv. Funct. Mater.*, 2014, **24**, 5261–5268.
8. K. K. Oehlenschlaeger, J. O. Mueller, J. Brandt, S. Hilf, A. Lederer, M. Wilhelm, R. Graf, M. L. Coote, F. G. Schmidt, C. Barner-Kowollik, *Adv. Mater.*, 2014, **26**, 3561–3566.
9. J. Canadell, H. Goossens, B. Klumperman, *Macromolecules*, 2011, **44**, 2536–2541.
10. W. M. Xu, M. Z. Rong, M. Q. Zhang, *J. Mater. Chem. A*, 2016, **4**, 10683–10690.
11. B. T. Michal, C. A. Jaye, E. J. Spencer, S. J. Rowan, *ACS Macro Lett.*, 2013, **2**, 694–699.
12. C. M. Chung, Y. S. Roh, S. Y. Cho, J. G. Kim, *Chem. Mater.*, 2004, **16**, 3982–3984.
13. P. Froimowicz, H. Frey, K. Landfester, *Macromol. Rapid Commun.* **2011**, **32**, 468–473.
14. B. Ghosh, M. W. Urban, *Science*, 2009, **323**, 1458–1460.
15. R. Cromwell, J. Chung, Z. B. Guan, *J. Am. Chem. Soc.*, 2015, **137**, 6492–6495.
16. Z. K. Wang, Q. M. Pan, *Adv. Funct. Mater.*, 2017, **27**, 1700690.
17. J. J. Cash, T. Kubo, A. P. Bapat, B. S. Sumerlin, *Macromolecules*, 2015, **48**, 2098–2106.
18. J. Liu, J. Liu, S. Wang, J. Huang, S. W. Wu, Z. H. Tang,; B. C. Guo, L. Q. Zhang, *J. Mater. Chem. A*, 2017, **5**, 25660–25671.
19. C. H. Li, C. Wang, C. Keplinger, J. L. Zuo, L. H. Jin, Y. Sun, P. Zheng, Y. Cao, F. Lissel, C. Linder, X. Z. You, Z. N. Bao, *Nat. Chem.*, 2016, **8**, 618–624.
20. S. Bode, L. Zedler, F. H. Schacher, B. Dietzek, M. Schmitt, J. Popp, M. D. Hager, U. S. Schubert, *Adv. Mater.*, 2013, **25**, 1634–1638.
21. D. Mozhdghi,; S. Ayala, O. R. Cromwell, Z. B. Guan, *J. Am. Chem. Soc.*, 2014, **136**, 16128–16131.
22. C. Wang, H. Wu, Z. Chen, M. McDowell, Y. Cui, Z. Bao, *Nat. Chem.*, 2013, **5**, 1042–1048.

23. J. Cao, C. H. Lu, J. Zhuang, M. X. Liu, X. X. Zhang, Y. M. Yu, Q. C. Tao, *Angew. Chem. Int. Ed.*, 2017, **56**, 8795–8800.
24. Y. L. He, S. L. Liao, H. Y. Jia, Y. Y. Cao, Z. N. Wang, Y. P. Wang, *Adv. Mater.*, 2015, **27**, 4622–4627.
25. M. Nakahata, Y. Takashima, H. Yamaguchi, A. Harada, *Nat. Commun.*, 2011, **2**, 511.
26. M. M. Zhang, D. H. Xu, X. Z. Yan, J. Z. Chen, S. Y. Dong, B. Zheng, F. H. Huang, *Angew. Chem.*, 2012, **124**, 7117–7121.
27. J. Liu, C. S. Y. Tan, Z. Yu, N. Li, C. Abell, O. A. Scherman, *Adv. Mater.*, 2017, **29**, 1605325.
28. S. Burattini, B. W. Greenland, W. Hayes, M. E. Mackay, S. J. Rowan, H. M. Colquhoun, *Chem. Mater.*, 2011, **23**, 6–8.
29. S. Burattini, B. W. Greenland, D. H. Merino, W. G. Weng, J. Seppala, H. M. Colquhoun, W. Hayes, M. E. Mackay, I. W. Hamley, S. J. Rowan, *J. Am. Chem. Soc.*, 2010, **132**, 12051–12058.
30. J. C. Lai, J. F. Mei, X. Y. Jia, C. H. Li, X. Z. You, Z. N. Bao, *Adv. Mater.*, 2016, **28**, 8277–8282.
31. E. Carrington, J. M. Gosline, *Am. Malacol. Bull.*, 2004, **18**, 135–142.
32. H. Lee, S. M. Dellatore, W. M. Miller, P. B. Messersmith, *Science*, 2007, **318**, 426–430.
33. N. Holten-Andersen, G. E. Fantner, S. Hohlbauch, J. H. Waite, F. W. Zok, *Nat. Mater.*, 2007, **6**, 669–672.
34. C. J. Sun, J. H. Waite, *J. Biol. Chem.*, 2005, **280**, 39332–39336.
35. S. Haemers, M. C. van der Leeden, G. Frens, *Biomaterials*, 2005, **26**, 1231–1236.
36. C. V. Benedict, J. H. Waite, *J. Morphol.*, 1986, **189**, 171–181.
37. J. Sedo, J. Saiz-Poseu, F. Busque, D. Ruiz-Molina, *Adv. Mater.*, 2013, **25**, 653–701.
38. N. Holten-Andersen, T. E. Mates, M. S. Toprak, G. D. Stucky, F. W. Zok, J. H. Waite, *Langmuir*, 2009, **25**, 3323–3326.
39. A. Avdeef, S. R. Sofen, T. L. Bregante, K. N. J. Am. Chem. Soc., 1978, **100**, 5362–5370.
40. H. Lee, N. F. Scherer, P. B. Messersmith, *P. Natl. Acad. Sci. USA*, 2006, **103**, 12999–13003.
41. N. Holten-Andersen, M. J. Harrington, H. Birkedal, B. P. Lee, P. B. Messersmith, K. Y. C. Lee, J. H. Waite, *P. Natl. Acad. Sci. USA*, 2011, **108**, 2651–2655.
42. M. J. Harrington, A. Masic, N. Holten-Andersen, J. H. Waite, P. Fratzl, *Science*, 2010, **328**, 216–220.
43. P. S. Yavvari, A. Srivastava, *J. Mater. Chem. B*, 2015, **3**, 899–910.
44. N. Chen, Q. M. Pan, *ACS Sustainable Chem. Eng.*, 2017, **5**, 7905–7811.
45. N. N. Xia, X. M. Xiong, J. H. Wang, M. Z. Rong, M. Q. Zhang, *Chem. Sci.*, 2016, **7**, 2736–2742.
46. G. E. Fantner, T. Hassenkam, J. H. Kindt, J. C. Weaver, H. Birkedal, L. Pechenik, J. A. Cutroni, G. A. Cidade,

- G. D. Stucky, D. E. Morse, *Nat. Mater.*, 2005, **4**, 612–616.
47. N. Becker, E. Oroudjev, S. Mutz, J. P. Cleveland, P. K. Hansma, C. Y. Hayashi, D. E. Makarov, H. G. Hansma, *Nat. Mater.*, 2003, **2**, 278–283.
48. E. Ducrot, Y. L. Chen, M. Bulters, R. P. Sijbesma, C. Creton, *Science*, 2014, **344**, 186–189.
49. Z. Shafiq, J. X. Cui, L. Pastor-Perez, V. San Miguel, R. A. Gropeanu, C. Serrano, A. del Campo, *Angew. Chem.*, 2012, **124**, 4408–4411.
50. V. M. Nurchi, T. Pivetta, J. I. Lachowicz, G. Crisponi, *J. Inorg. Biochem.*, 2009, **103**, 227–236.
51. M. S. Menyo, C. J. Hawker, J. H. Waite, *Soft Matter*, 2013, **9**, 10314–10323.
52. M. D. Shultz, J. U. Reveles, S. N. Khanna, E. E. Carpenter, *J. Am. Chem. Soc.*, 2007, **129**, 2482–2487.
53. D. G. Barrett, D. E. Fullenkamp, L. H. He, N. Holten-Andersen, K. Y. C. Lee, P. B. Messersmith, *Adv. Funct. Mater.*, 2012, **23**, 1111–1119.
54. Y. P. Ioshchenko, V. F. Kablov, G. E. Zaikov, *Russ. J. Appl. Chem.*, 2008, **81**, 1358–1364.
55. H. F. Pan, W. Wang, Y. Pan, L. Song, Y. Hu, K. M. Liew, *Carbohydr. Polym.*, 2015, **115**, 516–524.
56. G. Laufer, C. Kirkland, A. B. Morgan, J. C. Grunlan, *Biomacromolecules*, 2012, **13**, 2843–2848.
57. M. Rozanowska, T. Sarna, E. J. Land, T. G. Truscott, *Free Radical Biol. Med.*, 1999, **26**, 518–525.
58. J. H. Cho, V. Vasagar, K. Shanmuganathan, A. R. Jones, S. Nazarenko, C. J. Ellison, *Chem. Mater.*, 2015, **27**, 6784–6790.